

# Kinetics and Thermodynamics of Acid Red 1 Adsorption on Used Black Tea Leaves from Aqueous Solution

Rasel Ahmed<sup>1</sup>, Raisa Rahman Rafia<sup>2</sup>, Mohammad Abul Hossain<sup>2</sup> 

<sup>1</sup>Department of Chemistry, Pabna University of Science and Technology, Pabna-6600, Bangladesh

<sup>2</sup>Department of Chemistry, Faculty of Science, University of Dhaka, Dhaka-1000, Bangladesh

**Abstract:** This study presents the investigation of kinetics and thermodynamics of adsorption of Acid Red 1 (AR1) from aqueous solution on used black tea leaves (UBTL) as a biosorbent. The effects of initial dye concentration, solution pH and temperature on the adsorption kinetics were evaluated through batch adsorption experiments. Different kinetic model equations such as pseudo first order, pseudo second order, Elovic and Intra-particle diffusion were applied to the experimental data to evaluate their validity and determined their respective parameters. The results revealed that the adsorption kinetics is well described by pseudo second order kinetic equation. The equilibrium amounts adsorbed, calculated from the pseudo second order kinetic plots for different initial concentrations, were used to construct the adsorption isotherm which is well expressed by Langmuir equation compared with Freundlich one and the maximum adsorption capacity was 30.03 mg/g. Again, the equilibrium amounts adsorbed, calculated from the pseudo second order kinetic plots for different temperatures, were increased with the increase of adsorption temperature indicating the adsorption is endothermic. The calculated values of apparent activation energy ( $E_a = 3.35$  kJ/mol), enthalpy change ( $\Delta H = +30.05$  kJ/mol), entropy change ( $\Delta S = +0.119$  kJ/mol) and free energy change ( $\Delta G$ ) revealed that the adsorption of AR1 on UBTL at pH 2.0 was endothermic, spontaneous and physical in nature. The equilibrium amount adsorbed for different initial pH of solution, calculated from pseudo order kinetic plots, was found to be decreased with increase of solution pH from 2.0 to 8.0 suggesting the adsorption mechanism is dominated by electrostatic interaction between positive surface of UBTL at pH 2.0 and negative AR1 dye molecules.

**Keywords:** Acid Red 1, Used Black Tea Leaves, Adsorption Kinetics, Thermodynamics, Mechanism

## 1. Introduction

In the recent era, an important issue is the environmental pollution especially water pollution caused by industrial effluents. Industrial effluents contain various synthetic dyes used in industries for coloring purpose. All kinds of fabrics and baby food are colored using synthetic mono azo dyes like as acid red 1 (AR1) [1]. Various problems such as reduction of light penetration, reduction of oxygen solubility and photosynthetic activity for aquatic life caused due to presence of dyes in water [2]. Azo dyes are the most used dye among the dye compounds due to the diversity in chemical structure and easy to make these dyes [3]. These dyes are non biodegradable and more stable due to complex structure. Moreover, toxic and carcinogenic characteristic of dyes causes serious destruction on kidneys, liver, brain, fertility and central nerve system [4-5]. Hence, it is a dire need to maintain the quantity of colored dyes in waste liquids before its discharge into streams of water bodies.

In the last few years, for the remediation of dye from wastewater to control water pollution, various physical, chemical and biological methods were used. For instance: advanced oxidation [6-7], photodegradation [8], electrocoagulation [9], adsorption [10], anion exchange membrane [11], cation exchange membrane [12], coagulation/flocculation [13] are commonly used. Amongst all these removal methods, adsorption is the most widely used procedure due to its cost

effectiveness, simple design, easy operation and efficiency.

There are various types of adsorbent materials used in removing colored dyes from aqueous solutions effectively. Because of high and versatile adsorbent capability and microporous structure, activated carbon is highly recognized adsorbent for removing acid red 1 dye from waste water [14-15]. But, its commercial use is limited due to its high cost. This problem can overcome using non-conventional adsorbents such as chitosan-*iso*-vanillin sorbent material [10], spent mushroom waste [16], peel of cucumis sativus fruit [17], preformed floccs [18], used black tea leaves (UBTL) etc. Out of them, UBTL act as a good adsorbent in the adsorption study due to economically cheap, easily accessible, environment friendly, high adsorption capacity and easy to recover the adsorbate from adsorbed UBTL [19]. Therefore, the main objective of this study was to assess the potentiality of UBTL to remove Acid Red 1 (AR1) dye from synthetic wastewater. The impact of various parameters like initial dye concentration, solution pH and processing temperature were investigated.

## 2. Materials and Methods

### 2.1 Chemicals

All chemicals of analytical grade were used in this study. Acid red 1 (AR1) is the adsorbate in this research work which is a strong acid dye and anionic in nature. The chemical formula of this dye is  $C_{18}H_{13}N_3Na_2O_8S_2$  and molecular weight 509.42



g/mole. Its IUPAC name is (5-(Acetylamino)-4-hydroxy-3-(phenylazo) naph-thalene-2,7-disulphonic acid). The molecular structure of Acid Red 1 is shown in Figure 1. This dye contains sulfonic acid groups, which gives the dye molecule as a negative charge in aqueous media. Distilled water was used to prepare all the solutions for each experiment. The initial solution pH was adjusted using 0.1 M HNO<sub>3</sub> or 0.1 M NaOH.

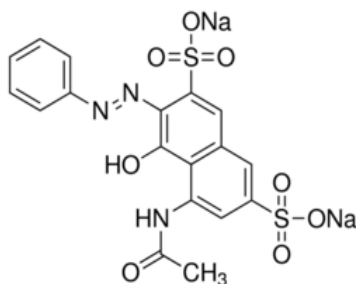


Figure 1 Molecular structure of Acid Red 1 (AR1)

## 2.2 Preparation of adsorbent

In the beginning of this study, fresh black tea leaves were collected from departmental store in Dhaka city, Bangladesh. To remove colored materials from fresh black tea leaves, about 50 g of fresh black tea leaves were boiled in 500 mL of distilled water for 2 hours. Then dried in oven at 105°C for 12 hours and prepared leaves were sieved through the metallic sieves of mesh size 212- 300 μm. Finally, stored in air tight bottle and kept in desiccators. The surface morphology of the prepared UBTL was investigated under Scanning Electron Microscopy (SEM) (JSM-6490LA, JEOL, Japan) and presented in Figure 2 which shows the heterogeneous surface morphology of prepared UBTL.

## 2.3 Experimental

In this study, the adsorption of AR1 from aqueous solution was investigated by executing batch adsorption experiments. At first, the experiment was carried out in a series of reagent bottles at a constant

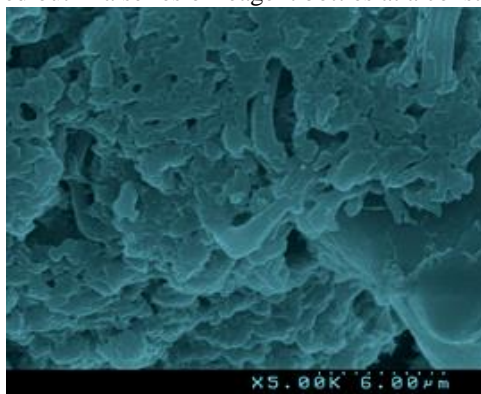


Figure 2 SEM micrograph of prepared UBTL×5000.

temperature to investigate the impact of initial concentration on adsorption process. 25.0 mL of fixed concentrated Acid Red 1 solution at pH 2.0 as a predetermined optimum pH was taken in each of 6 bottles and 0.0500 g of UBTL was added. Then solution was shaken in a thermostatic mechanical shaker (NTS-4000 Eyela, Japan) at 35.0±0.2°C. The mixtures were separated, after shaking of different time of intervals. Supernatant of each bottles were properly diluted and adjusted the pH at pH 6.0 using 0.1 M HNO<sub>3</sub> or 0.1 M NaOH and UV-vis spectrophotometer (Model-1800A, Shimadzu, Japan) was used to measure the absorbance at λ<sub>max</sub> 530.5 nm to determine the concentrations of AR1 in solutions after adsorption. Similarly, concentration of AR1 in initial solution was also determined at same pH 6.0. Similar kinetic experiments were performed using five different initial concentrations of Acid Red 1 solutions. The amount adsorbed at different contact times for different initial concentration was calculated from the following equation,

$$q_t = \frac{(C_o - C_t)V}{W} \quad (1)$$

where, C<sub>o</sub> = initial concentration of AR1 (mg/L), C<sub>t</sub> is the concentration of AR-1 at time *t* (mg/L), *q<sub>t</sub>* is the amount adsorbed at time *t* (mg/g). *V* is the volume of solution in Liter and *W* is the mass of adsorbent in g. Similar kinetic experiments were carried out at four different temperature values at constant pH (2.0) for fixed concentrated solution of 100 mg/L Acid Red 1. Similar kinetic experiments were also carried out at different pH values at constant temperature for fixed concentrated solution of 100 mg/L Acid Red 1.

## 3. Results and discussion

### 3.1 Effect of Concentration

The effect of dye concentration on adsorption kinetics was investigated by performing a series of kinetic experiments using various concentration of AR1 at constant temperature, solution pH, adsorbent dose and agitation rate. The concentration of AR1 in solution was decreased with time since AR1 dye adsorbed on the UBTL surface. The variation of amount adsorbed of AR1 with contact time for a fixed amount of adsorbent is increased as shown in Figure 3. The figure shows that the amount adsorbed is initially rapidly increased with increase in contact time and then becomes steady for different initial concentration of AR1 which is evaluated by different kinetic model equations as follows:

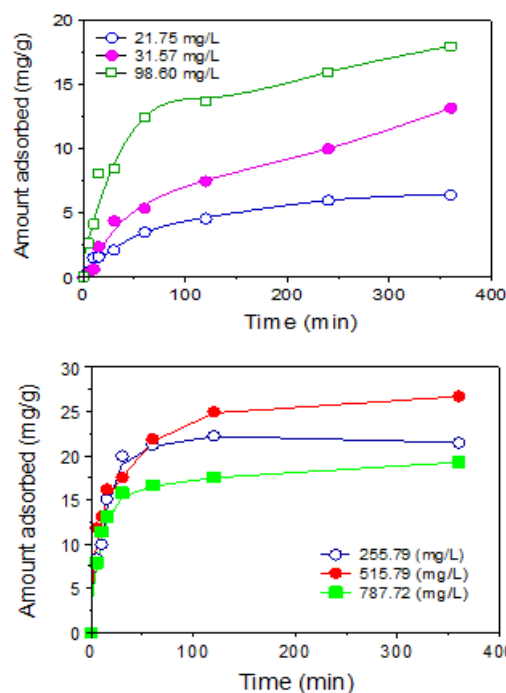


Figure 3 Variation of the amount adsorbed of AR1 on UBTL with time for different initial concentrations at pH 2.0 and at 35.0  $\pm 0.2^\circ\text{C}$ .

### 3.2 Kinetic Modeling on Adsorption Study

Different kinetic model equations such as pseudo first order, pseudo second order, Elovic model and Intra-particle diffusion model were applied to the kinetic data of dye adsorption onto used black tea leaves to investigate the dynamics of adsorption process.

#### 3.2.1 Pseudo first order kinetics

The adsorption kinetic data was investigated by applying pseudo first order kinetic equation given by Lagergren [22-24]. According to this model, one active site on surface occupied with one adsorbate species. The linearized form of the pseudo first order kinetic equation is expressed as following equation (2):

$$\ln(q_e - q_t) = \ln q_e - k_1 t \quad (2)$$

where,  $q_e$  and  $q_t$  are the adsorption capacity at equilibrium and at time  $t$ , respectively (mg/g),  $k_1$  is the rate constant of pseudo first order adsorption (L/min). Figure 4 shows that the pseudo first order kinetic equation as a plot of  $\ln(q_e - q_t)$  vs  $t$  is partially applicable for the adsorption of low concentrated AR1 on UBTL but is not applicable for the adsorption of high concentrated AR1 on UBTL. The values of regression coefficient ( $R^2$ ) for the applicability of pseudo first order kinetic equation to the experimental data are given in Table 1.

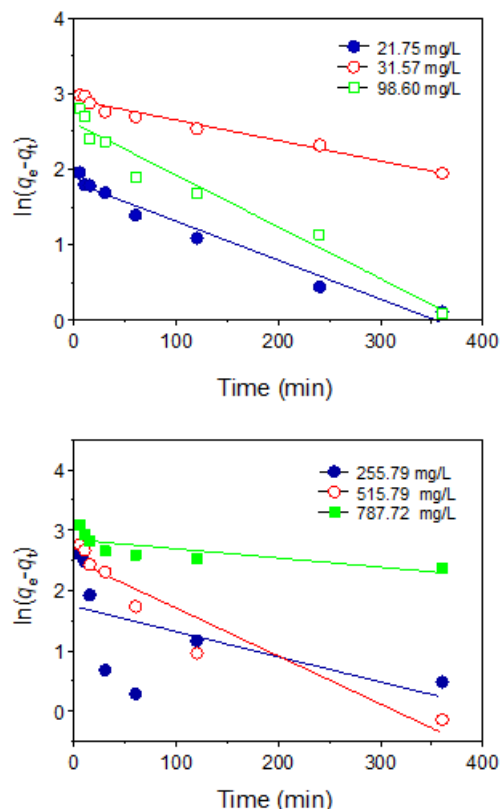


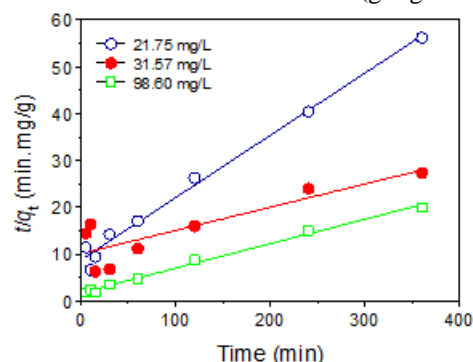
Figure 4 Pseudo first order kinetic plot of the adsorption of AR1 on UBTL at pH 2.0 and 35.0  $\pm 0.2^\circ\text{C}$  for different initial concentrations.

#### 3.2.2 Pseudo second-order kinetics

The pseudo second-order kinetic model describes the kinetic behavior of adsorption process on solid surfaces for the liquid–solid system [25-26]. Ho and McKay's pseudo second order rate equation linearly expressed as following:

$$\frac{t}{q_t} = \frac{1}{k_2 q_e^2} + \frac{t}{q_e} \quad (3)$$

where,  $q_t$  is the amount adsorbed at time  $t$  (mg/g),  $q_e$  is the equilibrium amount adsorbed (mg/g) and  $k_2$  is the pseudo second order rate constant (g/mg $\cdot$ min).



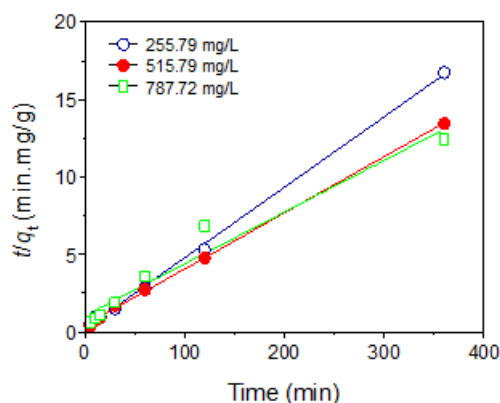


Figure 5 Pseudo second-order kinetic plot of the adsorption of AR1 on UBTL at pH 2.0 and  $35.0 \pm 0.2^\circ\text{C}$  for different initial concentrations.

Ho and McKay's pseudo second order rate equation (3) was verified by plotting  $t/q_t$  vs  $t$  as shown in Figure 5. The figure shows that each plot follows the straight line with the whole range of concentration indicating the fitness of pseudo second order rate equation for the adsorption of AR1 on UBTL in both at low and high concentration of AR1. The values of regression coefficient ( $R^2$ ) for the fitness of pseudo second order kinetic equations to the adsorption kinetics of different concentrated AR1 on UBTL at pH 2.0 are given in Table 1. From these straight lines of each plot the value of equilibrium amount adsorbed, equilibrium concentration and pseudo second order rate constant were calculated for different initial concentrations of AR1 and the values are given in Table 2.

### 3.2.3 Elovich model

Recently, several adsorption studies [16, 27] used the Elovich equation to describe the adsorption kinetics. The integrated form of Elovich equation is shown in Equation (4).

$$q_t = \frac{1}{\beta} \ln(\alpha\beta) + \frac{1}{\beta} \ln t \quad (4)$$

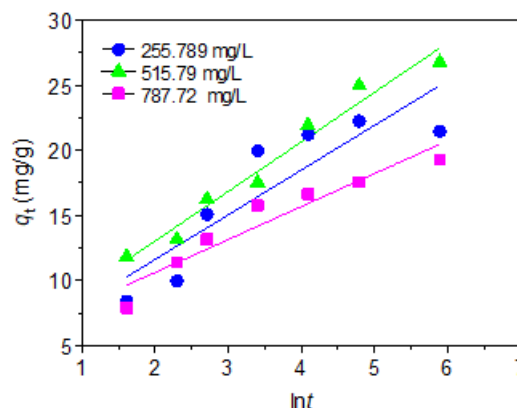
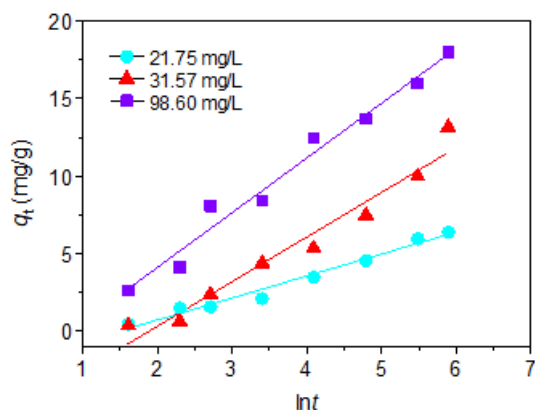


Figure 6 Elovich plot for the adsorption of AR1 on UBTL at pH 2.0 and  $35.0 \pm 0.2^\circ\text{C}$  for different initial concentrations.

where,  $\alpha$  is the initial adsorption rate ( $\text{mg/g} \cdot \text{min}$ ) and  $\beta$  is related to the extent of surface coverage and the activation energy for chemisorption ( $\text{g/mg}$ ). By applying the above equation (4), the adsorption of AR1 on UBTL for different initial concentrations were verified and the plot of  $q_t$  versus  $\ln t$  in Figure 6 shows that the adsorption of AR1 on UBTL does not follow the Elovich equation for different initial concentrations of AR1 at pH 2.0 and at  $35 \pm 0.2^\circ\text{C}$ . The values of regression coefficient ( $R^2$ ) for the applicability of Elovich equation to the experimental data are given in Table 1.

### 3.2.4 Intra-particle diffusion model

Weber's intraparticle diffusion model is widely used to investigate the diffusion mechanism of adsorption process [10, 18, 28]. Linear form of the intraparticle diffusion model is given by equation (5),

$$q_t = k_{id} t^{1/2} + C \quad (5)$$

where,  $q_t$  is the amount of color adsorbed per gram of adsorbent,  $t$  is the time of uptake,  $C$  is the intercept and  $k_{id}$  is the intraparticle diffusion rate constant ( $\text{mg/g} \cdot \text{min}^{1/2}$ ). The plot  $q_t$  versus  $t^{1/2}$  portrayed in Figure 7 reveals that each of the straight line did not pass through the origin. From this observation, it can be said that the intraparticle diffusion model is not the rate controlling step and other mechanism was involved in adsorption process. The results are in agreement with other works [29-30].

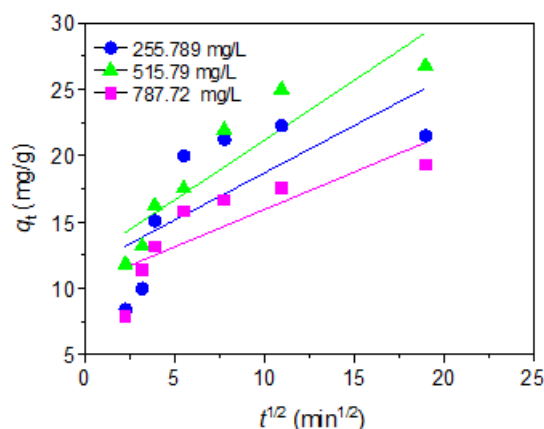
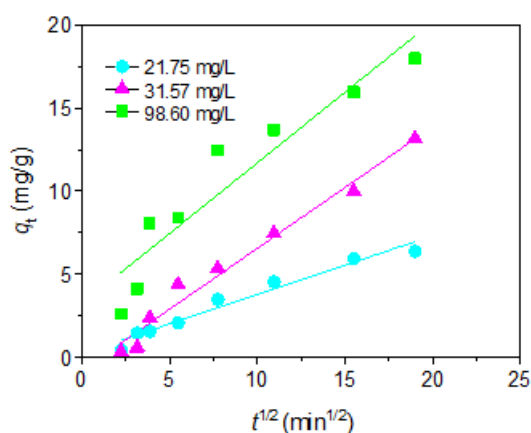
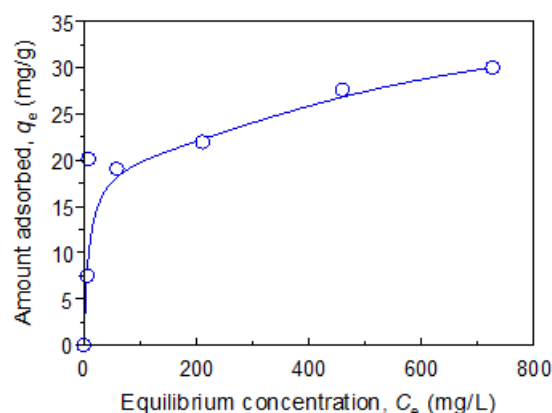
**Table 1:** A comparison of the data fitness to pseudo first, pseudo second order, elovic and intra-particle diffusion models.

Initial concentration $C_0$ (mg/L)	$R^2$ (-) pseudo first order	$R^2$ (-) pseudo second order	$R^2$ (-) Elovic model	$R^2$ (-) Intra-particle diffusion model
21.75	0.969	0.989	0.978	0.964
31.57	0.968	0.741	0.957	0.978
98.60	0.960	0.994	0.977	0.894
255.79	0.306	0.998	0.783	0.519
515.79	0.908	0.999	0.970	0.838
787.72	0.604	0.958	0.912	0.699

The adsorption kinetics of AR1 on UBTL at pH 2.0 can be evaluated by comparing the regression factor values (given in Table 1) for the fitness of pseudo first order, pseudo second order, Elovic and Intra-particle diffusion models. The low values of regression factor ( $R^2$ ) for the pseudo first order, Elovic and Intra-particle diffusion models show that these models poorly fitted the experimental data on the tested dyes. On the other hand, the pseudo second order model yielded the highest  $R^2$  values of all tested models. For this reason, the pseudo second order was found to best describe the adsorption process of the present study.

### 3.3 Adsorption Isotherm

Adsorption isotherm is very important to predict the adsorption capacities of the adsorbent at a particular condition. It describes the interactive behavior of adsorbate and adsorbent. Adsorption isotherm is the variation of amounts adsorbed ( $q_e$ ) on the surface of adsorbent with equilibrium concentration ( $C_e$ ) of adsorbate at constant temperature. The change of AR1 adsorbed at equilibrium with respect to equilibrium concentration of AR1 on UBTL is presented in Figure 8. In order to analyze the relationship between  $q_e$  and  $C_e$  two model equations of adsorption such as Langmuir and Freundlich isotherms were applied to the adsorption of AR1 over the surface of UBTL.


 Figure 7 Intra-particle diffusion model plots for the adsorption of AR1 on UBTL at pH 2.0 and  $35.0 \pm 0.2^\circ\text{C}$  for different initial concentrations.

 Figure 8 Adsorption isotherm of AR1 on UBTL at pH 2.0 and at  $35.0 \pm 0.2^\circ\text{C}$ 

#### 3.3.1 Freundlich isotherm

The Freundlich adsorption isotherm is an empirical equation for the adsorption takes place on a heterogeneous system as well as multilayer adsorption mechanism [31]. The linear form of Freundlich equation is mathematically given by the equation (6),

$$\log q_e = \log k_F + \frac{1}{n} \log C_e \quad (6)$$

where,  $C_e$  (mg/L) is the dyes concentration at equilibrium,  $q_e$  (mg/g) is the dyes adsorption capacity at equilibrium,  $k_F$  is the proportionality constant and  $n$  is considered as heterogeneity constant in literature. The plot of  $\ln q_e$  vs  $\ln C_e$  is shown in Figure 9 which is deviate from the straight line suggested failure of the Freundlich equation for this system.



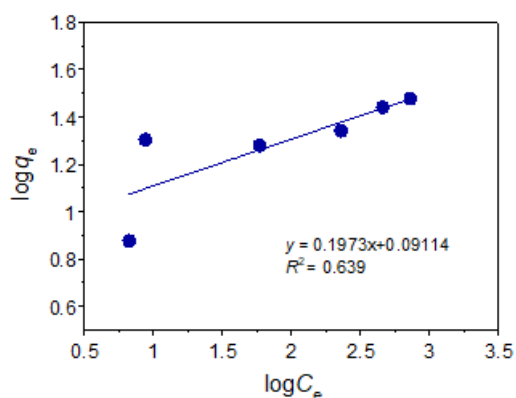


Figure 9 Freundlich isotherm for adsorption of AR1 on UBTL at pH 2.0 and at 35.0±0.2°C

### 3.3.1 Langmuir isotherm

Langmuir isotherm is derived by assuming the adsorption takes place on homogeneous surface [31]. The linear form of Langmuir equation is expressed as equation (7),

$$\frac{C_e}{q_e} = \frac{1}{q_m b} + \frac{C_e}{q_m} \quad (7)$$

where  $C_e$  (mg/L) is the dyes concentration at equilibrium,  $q_e$  (mg/g) is the dyes adsorption capacity at equilibrium,  $q_m$  (mg/g) is the maximum adsorption capacity for complete monolayer and  $b$  (L/mg) is the Langmuir constant related to adsorption equilibrium constant and the others parameters is previously described in Langmuir equation. A linear plot of  $C_e/q_e$  against  $C_e$  at 35.0±0.2°C, calculated from pseudo second order kinetic plots for different initial concentrations (Fig. 5), presented in Figure 10 which is unexpected straight line with high value of regression coefficient ( $R^2 = 0.998$ ). Such applicability of Langmuir equation to the adsorption of other dyes on heterogeneous surface of UBTL were reported in our previous studies [20, 21]. Thus the maximum adsorption capacity of UBTL to AR1 was calculated from the plot and the value,  $q_m = 30.03$  mg/g at pH 2.0.

### 3.4 Effect of Temperature on Adsorption kinetics

Temperature is one of the most important controlling parameter in the adsorption process. The influence of temperature on adsorption of AR1 on UBTL was verified in the temperature range 25 to 50 °C with same initial concentration of dye. The variation of amount adsorbed with time for different temperatures

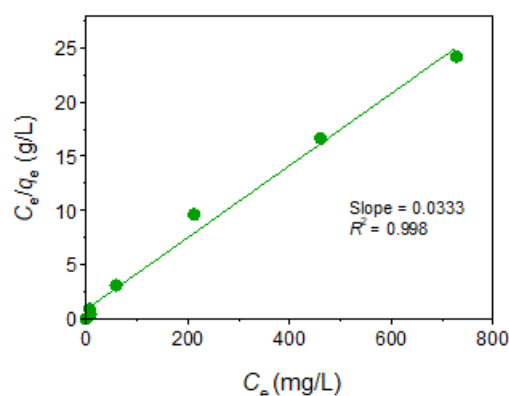


Figure 10 Langmuir isotherm for adsorption of AR1 on UBTL at pH 2.0 and at 35.0±0.2°C

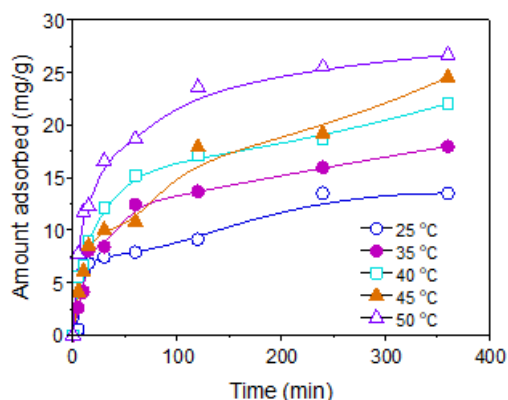


Figure 11 Change of the amount adsorbed with time during the adsorption of AR1 on UBTL at pH 2.0 for different temperatures.

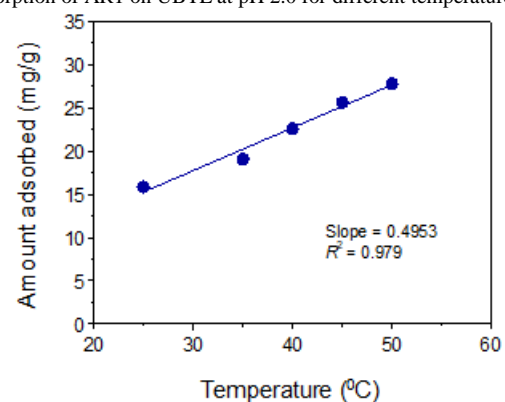


Figure 12 Variation of equilibrium amount adsorbed with temperature for adsorption of AR1 on UBTL at pH 2.0.

shown in Figure 11. Amounts adsorbed were calculated by applying pseudo second order kinetic plot (Fig. not shown) and its variation with temperature are presented in Figure 12. The figure reveals that with increasing temperature the amount adsorbed increased, indicating endothermic adsorption.

### 3.5 Thermodynamics of Adsorption

#### 3.5.1 Activation energy of adsorption

With the help of Arrhenius equation (8) [32], the apparent activation energy of adsorption was calculated from the pseudo second order rate constant

obtained at different temperatures.

$$\log k_2 = -\frac{E_a}{RT} + \log A \quad (8)$$

where,  $E_a$  is the apparent activation energy (kJ/mol),  $A$  is the Arrhenius temperature independent factor,  $k_2$  is the pseudo second order rate constant (g/mol·s) and  $R$  is the molar gas constant. The plot of  $\log k_2$  values at different temperatures against the reciprocal of absolute temperatures as shown in Figure 13. The apparent activation energy ( $E_a$ ) of the adsorption was calculated from the Arrhenius plot (Fig. 13) and the value was 3.35 kJ/mol, indicated the physical adsorption of the process. It has been reported that the value of apparent activation energy for chemisorption is in the range 65 - 250 kJ/mol [33].

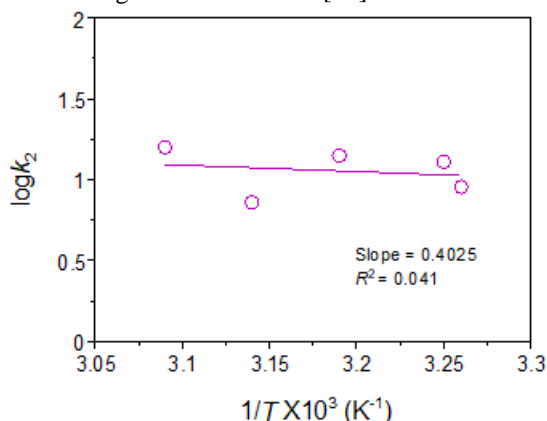


Figure 13 Arrhenius plot to determine the apparent activation energy of adsorption.

### 3.5.2 Thermodynamic parameters

The variation in dye removal efficiency with temperature can be explained using thermodynamic parameters such as enthalpy change ( $\Delta H_{ads}$ ), entropy change ( $\Delta S_{ads}$ ) and free energy change ( $\Delta G_{ads}$ ) [34]. The values  $\Delta H_{ads}$ ,  $\Delta S_{ads}$  and  $\Delta G_{ads}$  were calculated with the help of change of equilibrium constants with temperature [35]. The free energy change of the adsorption was calculated using equation (9):

$$\Delta G_{ads} = -RT \ln K_C \quad (9)$$

where,  $\Delta G_{ads}$  is the free energy change (kJ/mol),  $R$  is the molar gas constant (8.314 J/mol·K),  $T$  is the absolute temperature and  $K_C$  states the equilibrium constant ( $= C_a/C_e$ ),  $C_a$  is the equilibrium concentration of AR1 on UBTL surface (mol/L),  $C_e$  is the equilibrium concentration of the AR1 in solution (mol/L). The values of enthalpy change and entropy change can be calculated from equation (10),

$$\ln K_C = \frac{\Delta S_{ads}}{R} - \frac{\Delta H_{ads}}{RT} \quad (10)$$

The linear plot of  $\ln K_C$  vs  $1/T$  shown in Figure 14 yields the enthalpy ( $\Delta H_{ads}$ ) and entropy ( $\Delta S_{ads}$ ) values

from the slope and intercept, respectively. The values of  $\Delta G_{ads}$ ,  $\Delta H_{ads}$  and  $\Delta S_{ads}$  are listed in Table 2. The spontaneous nature of AR1 adsorption on UBTL and the feasibility of the method assured from the negative value of  $\Delta G_{ads}$ . The positive value of  $\Delta H_{ads}$  suggested that the adsorption is endothermic in nature. On the other hand, the positive value of  $\Delta S_{ads}$  confirms the increasing randomness at the solid/solution interface during the adsorption. All the findings of thermodynamic parameters are in agreement with earlier research findings [27, 36-38].

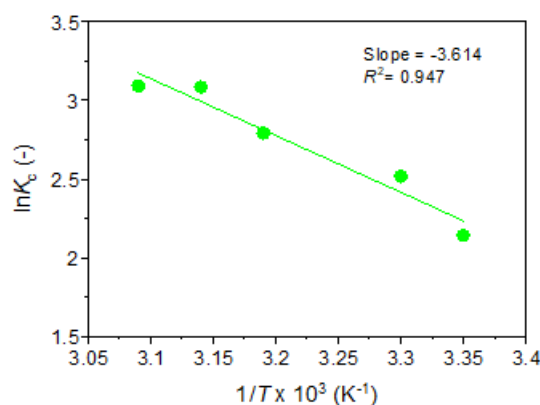


Figure 14 A plot of  $\ln K_C$  vs  $1/T$  for the determination of thermodynamic parameter during the adsorption of AR1 on UBTL.

**Table 2:** Adsorption equilibrium constant and thermodynamic parameters for AR1 adsorption on UBTL at different temperatures

T (K)	$\ln K_C$ (-)	$\Delta H_{ads}$ (kJ/mol)	$\Delta G_{ads}$ (kJ/mol)	$\Delta S_{ads}$ (kJ/{mol·K})
298	2.144	+ 30.05	-5.312	+ 0.119
303	2.518		-6.343	
313	2.794		-7.271	
318	3.087		-8.162	
323	3.094		-8.309	

### 3.6 Impact of pH on Adsorption Kinetics

It is usually recognized that adsorption process and adsorption capacity may be affected by the pH of dye solution [39]. Moreover, due to its impact on both the ionization process of the dye molecule and the surface binding sites of the adsorbent, the pH of dye solution is one of the crucial factors in the adsorption process [40]. The effect of pH on AR1 dye adsorption on UBTL was studied. Figure 15 shows the variation of amount adsorbed with time for different solution pH. The equilibrium amounts adsorbed for different initial pH of solutions was determined from pseudo second order kinetics plot. It has shown that the amount of AR1 adsorbed decreased with increasing pH of the dye solution from 2.0 to 8.0, presented in Figure 16. It has been reported that the AR1 dye is dissociated in an aqueous solution to produce the anion form. As result, the removal is well accomplished in acidic condition, due to the electrostatic attraction between the protonated adsorbent surface and the negative sulfonated groups of the dissociated dye molecules [41]. On the other hand, the removal of dye is

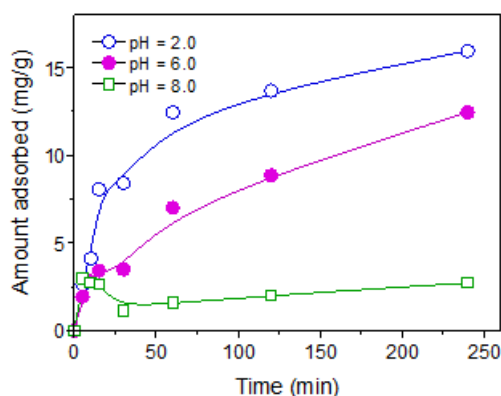


Figure 15 Change of the amount adsorbed of AR1 with time for different pH with initial concentration of 100.0 mg/L at 35.0±0.2°C.

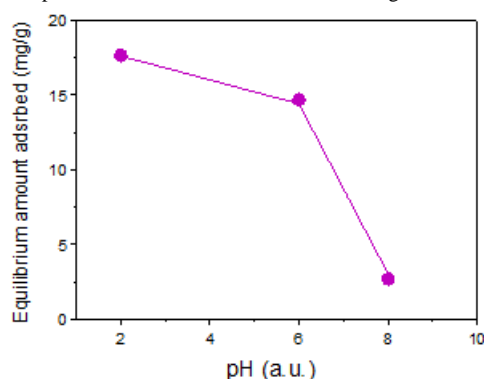


Figure 16 Variation of equilibrium amount adsorbed with pH for the absorption of AR1 on UBTL at 35.0±0.2°C.

decreased at high pH values because of the competition with hydroxyl ions that restricted the oncoming of dye anions [10].

#### 4 Conclusions

Adsorption of AR1 dye on UBTL is influenced by dye concentration, processing temperature and pH of solution. Kinetic study of adsorption revealed that the adsorption of AR1 on follows pseudo second kinetic equation and equilibrium data follows Langmuir isotherm. Apparent activation energy of adsorption, calculated from Arrhenius plot, indicated the physical adsorption of the process. Additionally, thermodynamic parameters such as free energy change, enthalpy change and entropy change suggested that the adsorption of AR1 on UBTL was spontaneous, feasible and endothermic in nature. Furthermore, with increase of solution pH, the equilibrium amount adsorbed was found to be decreased, indicating electrostatic interaction dominant the adsorption process. Finally, this study pointed out that UBTL is a promising low cost adsorbent for the removal of AR1 dye from aqueous solutions.

#### Acknowledgements

The authors would like to thank to Dhaka University-UGC Research Grant for partial support to complete the study. The authors also grateful to the department of Chemistry, University of Dhaka for given facilities

to performed the research work.

#### References

- Huitel, C. A. M., & Brillas, E. (2009) Decontamination of wastewaters containing syn-thetic organic dyes by electrochemical methods: A general review. *App. Catalysis B: Environ.* **87**(3-4), 105-145.
- Imran, M., Islam, A. U., Tariq, M. A., Siddique, M. H., Shah, N. S., Khan, Z. U. H., Amjad, M., Din, S. U., Shah, G. M., Naeem, M. A., Nadeem, M., Nawaz, M. & Rizwan, M. (2019) Synthesis of magnetite-based nanocomposites for effective removal of brilliant green dye from wastewater. *Environ. Sci. and Pollution Res.* **26** (24), 24489–24502.
- Chaleshtori, A. A. N., Meghaddam, F. M., Sadeghi, M. M., Rahimi, R. R., Hemati, S., Ahamadi, A. A., (2017) Removal of Acid Red 18 (Azo-Dye) from Aqueous Solution by Adsorption onto Activated Charcoal Prepared from Almond Shell. *J. of Environ. Sci. and Management* **20** (2), 9-16.
- Dincer, A. R., Gunes, Y., Karakaya, N., Gunes, E., (2007) Comparison of activated carbon and bottom ash for removal of reactive dye from aqueous solution, *Bioresource Technol.* **98**, 834-839.
- Shen, D., Fan, J., Zhou, W., Gao B., Yue, Q., & Kang, Q. (2009) Adsorption kinetics and iso-therm of anionic dyes onto organo-bentonite from single and multisolute systems. *Journal of Hazardous Materials*, **172** (1), 99-107.
- Deshannavar, U. B., Singa, P. K., Gaonkar, D., Gayathri, A., Patil, A., Malade, L.V., (2020) Removal of Acid Violet 49 and Acid Red 88 dyes from Aqueous Solutions using Advanced Oxidation Process. *Materials Today: Proceedings*, **20**(2), 1011-1019.
- Nemr, A. E., Hassaan, M., Madkour, F. F., (2018) Advanced Oxidation Process (AOP) for Detoxification of Acid Red 17 dye Solution and Degradation Mechanism. *Environ. Processes* **5** (1), 95-113.
- Jorfi, S., Barkhordari, M. J., Ahmadi, M., Jaafarzadeh, N., Moustofi, A., Ramavandi, B., (2018) Photodegradation of Acid red 18 dye by BiOI/ZnO nanocomposite: A dataset. *Data in Brief* **16**, 608-611.
- Amri, N., Abdullah, A. Z., Ismail, S., (2020) Removal Efficiency of Acid Red 18 Dye from Aqueous Solution Using Different Aluminium-Based Electrode Materials by Electrocoagulation Process. *Indones. J. Chem.* **20** (3), 536 – 544.
- Al-Abbad, E., Alakhras, F., (2020) Removal of Dye Acid Red 1 from Aqueous Solutions Using Chitosan-iso-Vanillin Sorbent Material. *Indones. J. of Sci. & Technol.* **5** (3), 352-365.
- Khan, M. A., Khan, M. I., and Zafar, S., (2017) Removal of different anionic dyes from aqueous solution by anion exchange membrane. *Membrane Water Treatment*, **8** (3), 259-277.
- Wu, J. S., Liu, C. H., Chu, K. H., Suen, S. Y., (2008) removal of Cationic Dye Methyl Violet 2B from Water by Cation Exchange Membranes. *J. of Membrane Sci.* **309** (1), 239-245.
- Zonoozi, M. H., Moghaddam, R. A., Arami, M., (2008) Removal of Acid Red 398 Dye from Aqueous Solutions by Coagulation/Flocculation Process. *Environ. Eng. and Management J.* **7** (6), 695-699.
- Aboushloa, E. M., and Etoriki, A. M., (2015) Removal of Synthetic Dye Acid Red 186 from Water by Activated Carbon. *British J. of Environ. Sci.* **3** (6), 54-64.
- Shokoohi, R., Vatanpoor, V., Zarrabi, M., AKRAM Vatani, A., (2010) Adsorption of Acid Red 18 (AR18) by Activated Carbon from Poplar Wood- A Kinetic and Equilibrium Study. *E-J. of Chem.* **7** (1), 65-72.
- Alhujaily, A., Yu, H., Zhang, X., Ma, F., (2020) Adsorptive removal of anionic dyes from aqueous solutions using spent mushroom waste. *App. Water Sci.* **10** (183), 1-12.
- Khanna, S., Rattan, V. K., (2017) Removal of Acid Red 1 from Aqueous Waste Streams using Peel of Cucumis Sativus Fruit: Equilibrium Studies. *J. of Chem. Technol. and Met.* **52** (5), 803-811



18. Munilakshmi, N., Srimuralia, M. and Janakiram Karthikeyana, J., (2013) Adsorptive Removal of Acid Red 1, from Aqueous Solutions by Preformed Floccs. *Int. J. of Current Eng. and Technol.* **3** (4), 1456-1462.
19. Hossain, M. A. (2006) Study on the process development for removal of Cr (VI) from waste water by sorption on Used Black Tea Leaves. (Doctoral Dissertation) Kanazawa University, Japan
20. Hossain, M. A., Hasan, T. A., Hossain, L., (2015) Adsorption of crystal violet on used black tea leaves from acidic solution: Equilibrium, Thermodynamic and Mechanism Studies. *Int. J. of Sci.* **4**(10), 31-39.
21. Hossain, M. A. and Hassan, M. T. (2013) Kinetic and thermodynamic study of the adsorption of Crystal Violet on used black tea leaves, *Orbital: Electron. J. Chem.* **5**(3), 148-156.
22. Lagergren, S. (1898) About the theory of so called adsorption of soluble substances, *Kungliga svenska vetenskapsakademiens. Handlingar*, **24**(4), 1-39.
23. Yilidiz, A., (2017) Adsorption of Acid Red 114 onto Fe<sub>3</sub>O<sub>4</sub>@Caffeic acid Recyclable Magnetic Nanocomposite. *J. of Turkish Chem. Soc.* **4** (1), 327-340.
24. Pang, X. Y., and Gong, F., (2008) Study on the Adsorption Kinetics of Acid Red 3B on Expanded Graphite. *E-J. of Chem.* **5** (4), 802-809.
25. Ho, Y. S., & McKay, G. (1999) Pseudo-second order model for sorption processes. *Process Biochemistry*, **34**, 451- 456.
26. Al-Arfaj, A. A., Alakhras, F., Al-Abbad, E., Alzamel, N. O., Al-Omair, N. A., & Ouerfelli, N. (2018) Removal of orange 2G dye from aqueous solutions using-based nanoparticles: isotherm and kinetic studies. *Asian J. of Chem.* **30**(7), 1645-1649.
27. Hossain, M. A., Ahmed, R., (2015) Kinetics and Thermodynamics of adsorption for the removal of Fast Green by used black tea leaves from aquatic environment, *British J. Env. Sci.* **3**(5), 32-44.
28. SriChandana, P., and Karthikeyan, J., (2012), Sorptive removal of color from aqueous coffee and tea infusions. *J. of Desalination and Water Treatment*, **50**, 338-347.
29. Jain, S. N., Gogate, P.R., (2017) Adsorptive removal of acid violet 17 dye from wastewater using biosorbent obtained from NaOH and H<sub>2</sub>SO<sub>4</sub> activation of fallen leaves of *Ficus racemosa*. *J. Mol. Liq.* **243**, 132-143.
30. Lafi R., Hafaiane, A., (2016) Removal of methyl orange (MO) from aqueous solution using cationic surfactants modified coffee waste (MCWs). *J. Taiwan Inst. Chem. Eng.* **58**, 424-433.
31. Eftekhari, S., Habibi-Yangjeh, A., Sohrabnezhad, S., (2010) Application of AlMCM-41 for competitive adsorption of methylene blue and rhodamine B: thermodynamic and kinetic studies. *J. Hazard. Mater.* **178**, 349
32. Bayramoglu, G., Altintas, B., Arica, M. Y., (2009) Adsorption kinetics and thermodynamic parameters of cationic dyes from aqueous solutions by using a new strong cation- exchange resin. *J. Chem. Eng.* **152**, 339-346.
33. Yu, Y., Zhuang, Y.Y., Wang, Z.H. (2001) Adsorption of water soluble dye onto functionalize resin. *J. Colloid Interf. Sci.* **242**, 288-293.
34. SriLakshmi, C., Saraf, R., (2016) Ag-doped hydroxyapatite as efficient adsorbent for removal of Congo Red dye from aqueous solution: synthesis, kinetic and equilibrium adsorption isotherm analysis. *Microporous Mesoporous Mater.* **219**, 134-144.
35. Haddad, M. E., (2012) Kinetic and thermodynamic studies on the adsorption behavior of Rhodamine B dye onto animal bone meal. *J. of Chem. Eng. and Mat. Sci.* **3**(3), 38-44.
36. Wu, K., Pan, X., Zhang, J., Zhang, X., Zene, A. S., Tian, Y., (2020) Biosorption of Congo Red from Aqueous Solutions Based on Self- Immobilized Mycelial Pellets: Kinetics, Isotherms, and Thermodynamic Studies. *ACS Omega*, **5**, 24601-24612.
37. Gedam, V. V., Raut, P., Chahande, A., Pathak, P., (2019) Kinetic, thermodynamics and equilibrium studies on the removal of Congo red dye using activated teak leaf powder. *App. Water Sci.* **9** (55), 1-13.
38. Oyelude, E. O., Awudza, J. A. M., & Twumasi, S. K., (2017) Equilibrium, Kinetic and Thermodynamic Study of Removal of Eosin Yellow from Aqueous Solution Using Teak Leaf Litter Powder. *Scientific Reports*, **7**, 1-10.
39. Zhou, Y., Ge, L., and Fan, N., (2018) Adsorption of Congo red from aqueous solution onto shrimp shell powder. *Adsorption Sci. & Technol.* **36** (5-6), 1310-1330.
40. Lafi, R., Montasser, I., Hafaiane, A., (2019) Adsorption of congo red dye from aqueous solutions by prepared activated carbon with oxygen-containing functional groups and its regeneration. *Adsorption Sci. & Technol.* **37** (1-2), 160-181.
41. Khanna, S., & Rattan, V.K. (2017) Removal of acid red 1 from aqueous waste streams using peel of cucumid sativus fruit: Equilibrium studies. *J. of Chem. Technol. and Met.* **52** (5), 803-811.